Morphology and bonding analysis of torrefied empty fruit bunch materials

Muhammad Iqbal Ahmad [1, 2, *], Nur Afiqah Bakri [3], Zairi Ismael Rizman [4], Mohd Sukhairi Mat Rasat [1], Zainal Alimuddin Zainal Alauddin [2], Shahril Nizam Mohamed Soid [5], Mohd Sharizal Abdul Aziz [2], Mazlan Mohamed [1], Mohamad Faiz Mohd Amin [3]

[1]*Faculty of Bioengineering and Technology, Universiti Malaysia Kelantan, 17600 Jeli, Kelantan, Malaysia*
[2]*School of Mechanical Engineering, Universiti Sains Malaysia, Engineering Campus, 14300 Nibong Tebal, Pulau Pinang, Malaysia*
[3]*Faculty of Earth Science, Universiti Malaysia Kelantan, 17600 Jeli, Kelantan, Malaysia*
[4]*Faculty of Electrical Engineering, Universiti Teknologi MARA, 23000 Dungun, Terengganu, Malaysia*
[5]*Malaysian Spanish Institute, Universiti Kuala Lumpur, 09000 Kulim, Kedah, Malaysia*

ARTICLE INFO

ABSTRACT

This study was conducted to investigate the impact of torrefaction process on surface morphology as well as functional group of EFB before undergoing further processing method so that it can be used as renewable energy. Scanning Electron Microscope (SEM) showed surface structure of EFB after undergoing torrefaction by which it is completely decomposed internally by producing pores, while the structure become flattened with almost disappeared sharp edge compared to the raw EFB. The changes of presence functional groups before and after the particular torrefaction process were observed under certain wavelength by using Fourier Transformation Infrared (FTIR) which were O-H bonds around 3420 cm^{-1}, C-H bonds around 2930, 1430 and 850 cm^{-1}, C=O bonds at 1750 cm^{-1} and much more.

1. Introduction

The depletion of fuel will lead to the environmental issues such as economic activities and rapid climate change, hence to remedy these issues, exploration and study of finding alternatives to fuels had come to renewable energy resources. Renewable energy is defined as any energy sources that are derived from solar energy (Sathaye and Meyers, 2013; Mohamed et al., 2015). Chen et al. (2012) listed that the renewable energy resources as such solar, ocean, wind, biomass, geothermal and hydropower. There are many energy sources which are biomass, coal, hydro, nuclear and wind power which play as a key role in generating energy with sustainability to the massive populations in developing countries (Painuly, 2001). According to Basu (2013), biomass is a promising alternative as it can provide a full range of feedstock accounted to replace 10% of world's annual energy consumption (IEA, 2010). The zero of net carbon emissions released from biomass burning (Chen et al., 2012) made it considerable as carbon neutral fuel (Ahmad et al., 2015). Moreover, its huge resources in global

scale, and the ability to be convert into thermal energy in forms of liquid, solid or gaseous fuels and other by-products. Biomass is defined as organic materials that originated from plants and animals (Loppinet et al., 2008). Formation of biomass from dead animals happened as microorganisms breaking down the biomass into water (H_2O), carbon dioxide (CO_2) and potential energy whereas biomass from plants are obtained by a photosynthesis process whereby carbon dioxide is converted into glucose in the presence of sunlight and water (Basu, 2013).

In this study, empty fruit bunch (EFB) is used that are obtained from waste removal of fruits or nuts from fruit bunches (Hakeem et al., 2015; Law et al., 2007) and in this case it is from oil palm fruit bunch due to its abundances which are one third of oil palm waste compared to oil palm fronds (OPF) and oil palm trunks (OPT) (Awalludin et al., 2015; Koguleshun et al., 2015). Other than EFB, OPF and OPT, mesocarp fiber (MF) and palm-kernel shells (PKS) are produced too as a by-products of oil extraction process (Uemura et al., 2013).

Every biomass including EFB will undergo several pretreatment processes before being a further processing as renewable energy. The pretreatment process composed of carbonization, gasification, pyrolysis and torrefaction. The more preferable process among those is torrefaction due to its production of coal substitute from biomass, which

caught the attention of power industries (Basu, 2013).

Torrefaction is stated as thermochemical process in an inert ambient, whereby biomass is gradually heated in a specific range of temperature between 200 to 300 ℃ (Bergman and Kiel, 2005) under an atmospheric pressure and characterized by a low heating rates of particle (< 50 ℃) (Basu, 2013) within a time less than 60 minutes. The properties of torrefied biomass EFB is further analyzed in terms of morphology and its bonding. In terms of morphology, torrefaction process change its structure in terms of particle sizes and structures look (Cruz et al., 2012; Ibrahim et al., 2013; Hamzah et al., 2013). Meanwhile, in terms of its bonding, different wavelength associates with different types of functional group that exists in EFB.

2. Methodology

2.1. Materials

Empty fruit bunches (EFB) which was derived from oil palm wastes of oil palm (Elaeis guineensis sp.) at an oil palm plantation in Felda Kemahang, Tanah Merah, Kelantan. EFB is chosen due to its potential as renewable biomass since it is locally produced in Malaysia and rich with lignocellulosic components (cellulose, hemicellulose and lignin) (Pua et al., 2011; Zakaria et al., 2013). The sample was grind and sieved into a smaller size. Later on, it was dried in an oven for an overnight.

2.2. Setup

Torrefaction process was carried out in an ambient pressure using a manual microwave oven; model Daewoo KO6L77 with maximum power of 700 W with dual wave system as a reactor. The experimental set-up was shown in Fig. 1. The torrefaction process required an inert gas to create a non-oxidizing environment by using nitrogen gas. Nitrogen (N2) gas was used to prevent oxidation and ignition in the microwave compared to oxygen (Tumuluru et al., 2010). Flow rate of N2 gas is 15 mLmin-1. N2 gas helped releasing gases from the sample upon torrefaction takes place in terms of both liquid and gas products (Ismail et al., 2013). EFB sample was placed in an alumina crucible and put inside the microwave (Ahmad et al., 2016). Parameters considered in this research were temperature, heat input (power) and residence time. Temperature is controlled using temperature controller (Abdullah et al., 2016; Rizman et al., 2013). The final product of torrefaction is torrefied material of EFB.

2.3. Sample analyses

Surface morphology and bonding of torrefied EFB were analyzed by using Scanning Electron Microscope (SEM), model JEOL JSM6360 LA and Fourier Transformation Infrared (FTIR), model Nicolet iN10 FTIR microscope respectively. Not only the torrefed EFB was analyzed, its raw also undergo the same analysis (Kassim et al., 2015), so that a comparison can be made.

3. Results and discussion

3.1. Surface morphology of EFB

Structure of EFB was perceived using scanning electron microscope (SEM) under magnifications of ×700; ×2000 and ×10000 were shown in Figs. 1-4 respectively. Raw EFB as shown in Fig. 1 indicates a smooth surface with sharp edges at the end (Figs. 1a and 1b). An unorganized and irregular fibers arrangement could be seen at its cross-sectional area (Figs. 1b and 1c). There were possibilities of pores, voids or inter-particle gaps presence in the structure of raw EFB, but they were not clearly determined due to the irregular fiber arrangements.
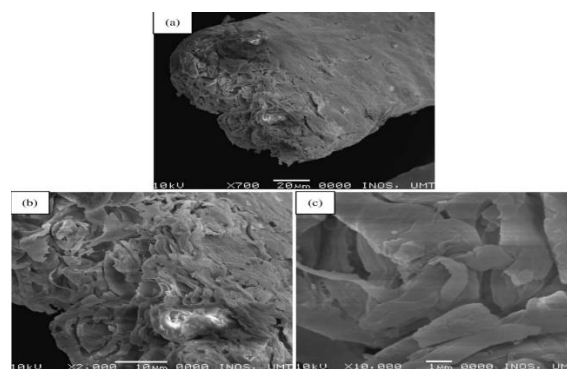

Fig. 1: Structure of raw EFB sieved 500 μm. (a) ×700 magnification, (b) ×2000 magnification and (c) ×10000 magnification

When compared to the torrefed EFB shown in Figs. 2-4 respectively, spongy-like structure was shown as the effect of torrefaction process. Fig. 2 shows the 20 minutes' residence time of torrefaction process where at the formation of porous were observed and determined. In Figs. 2a, 2b, and 2c, only torrefied EFB at 200°c shows a similar structure as raw EFB. This was because of the low temperature was used in the torrefaction process which almost unaffected the structure. Started at temperature of 225°c as shown in Figs. 2d, 2e, and 2f), interparticle gaps were formed but the sharp edge between the gaps were not completely diminished. The sharp edge became completely flattened at the torrefaction temperature of 250°c.

As the temperature increased corresponded with residence time upon torrefaction process take place, the structures of EFB became fully porous as shown in Fig. 3 and Fig. 4.

On a high magnification of ×2000 and ×10000, tiny particles could be clearly seen which were attached to the porous-structure of EFB. These were happening due to the particles of alumina crucible which were crack as the effect from thermal expansion happened inside it, causing alumina

unable to retain strength as temperature increased upon time. Mertke and Aneziris (2015) claimed that alumina crucible could retain strength when the thermal shock was 14.51 MPa at relatively high maximum temperature of 500 °c. However, frequently used alumina crucible could trigger the crack formation. Hence, causing its particles is attached to the structure.
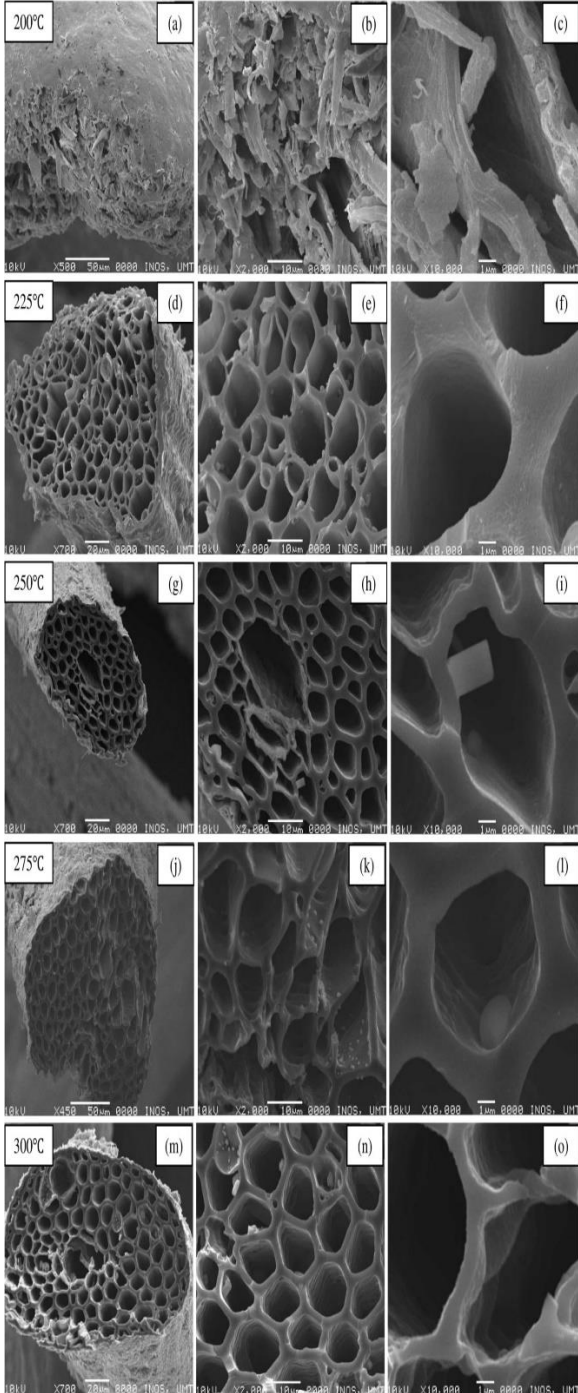

Fig. 2: Structure of torrefied EFB on 20 minutes of torrefaction at respective temperatures with magnifications of ×700 (a, d, g, j, m), ×2000 (b, e, h, k, n) and ×10000 (c, f, i, l,o)

Fig. 4 exposing a clear image of ruptured at the surface structure of the EFB from cross-sectional area's point of view. The ruptured images could be seen during 40 minutes of residence time (Fig. 3),
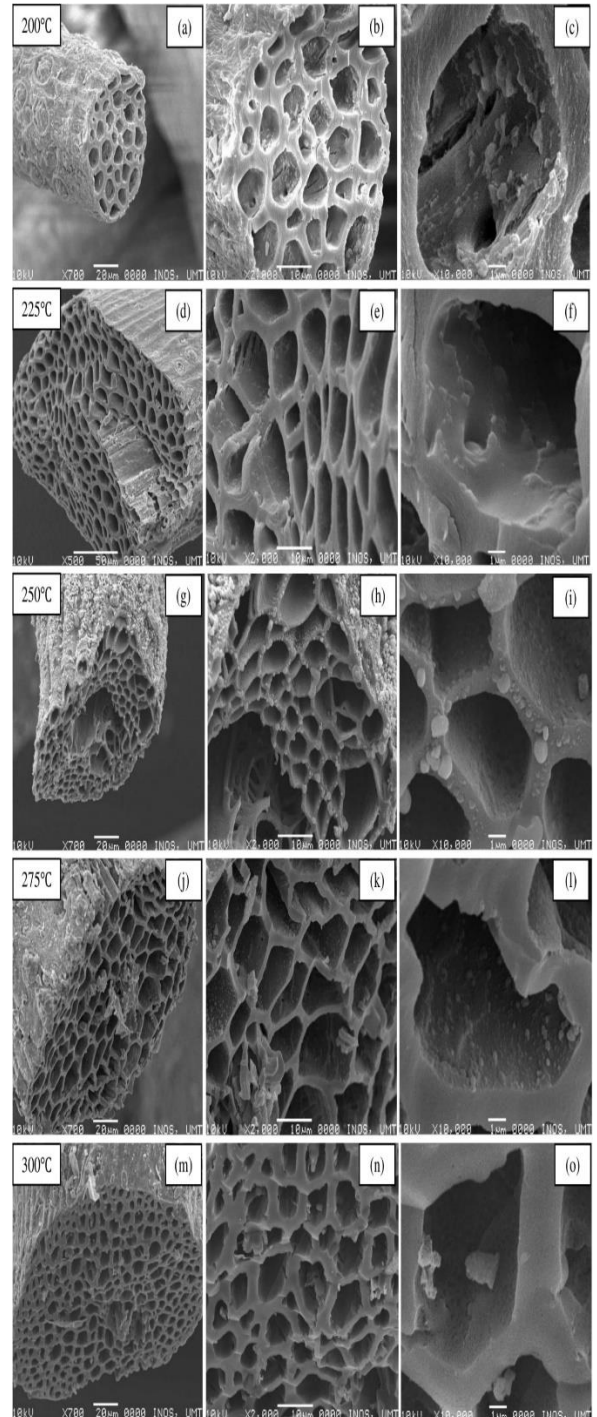
but not as clear as torrefaction's residence time of 60 minutes.

Fig. 3: Structure of torrefied EFB on 40 minutes of torrefaction at respective temperatures with magnifications of ×700 (a, d, g, j, m), ×2000 (b, e, h, k, n) and ×10000 (c, f, i, l, o)

The stretching of ruptured surface structures was caused by the degradation of lignocellulose compared to during the low temperature at low residence time. The clause of breakage of fiber wall surface was contributed by the rupture impact as the decomposition of cellulose and hemicellulose take places. Also, the ruptured images contributed to the degradation of lignocellulose, the porosity also participated in the degradation. High porosity indicates high degradation of lignocellulose. Longer

residence time causing a large amount of hemicellulose and cellulose were destroyed. Since the cellulose was degraded, the fiber wall became thinner as residence time was longest, 60 minutes. This was because of cellulose tending losing its strength. The longer the residence time, the faster the degradation happened as well as the temperature. When looked up closely at ×10000 magnification, the fiber was torn apart. Each of hemicellulose, cellulose and lignin were depleted underneath a certain temperature of torrefaction (Wen et al., 2014), whereby hemicellulose was decomposed at very low temperature started at 200 °C and completely disappeared as it almost reached 300 °C (Chen and Kuo, 2011b). Temperature above 250 °c was placed for cellulose degradation, whereas for lignin was on high temperature of 300 °c. Decomposition of lignin take place at high temperature and residence time respectively, because of its complex structure consists of phenolic polymer that made them strong and durable against an enzymatic attack (Gomez et al., 2008). Thus, lignin was hard to be degraded.

3.2. Fourier transforms infrared spectra

Fourier Transformation Infrared (FTIR) spectrometry been used in this studied to distinguish the change in chemical structure for both raw and torrefied EFB by analyzed the functional groups, which later on will affected the degradation of hemicellulose, cellulose and lignin as of torrefaction impact. Generally, studying the functional group helped in determined the frequency of each lignocellulose to be degenerated. Figs. 5-7 show the functional groups presence during 20 minutes, 40 minutes and 60 minutes of torrefaction respectively for selected torrefied EFB at temperature of 200 °c, 250 °c and 300 °c and being compared to the raw EFB. According to Nasri et al. (2013), absorption bands around 850-890 cm^{-1} indicated the deformation of C-H bending. Meanwhile, bands between 1045 up to 1055 cm^{-1} corresponded to the increasing of C-O stretching. Whereas, peaks ranged at 1430-1440 cm^{-1} show rapid stretch of C-H bond. On these bands, C-H_2 shearing and benching present. Bands of 1730-1750 cm^{-1} stating the C=O stretching take place. Both C-H and C-H_2 bonds appeared around bands of 2930-2950 cm^{-1}, but the bonding was stretched as the temperature of torrefaction increasing whereby the reaction of C-H was almost complete. The bands around 3420-3435 cm^{-1} were assigned for O-H stretching with rapid decreasing intensity. C-O-C stretching bond also identified at the band of 1260 cm^{-1}.

Based on these wavenumbers of infrared spectra, the degradation of hemicellulose, cellulose and lignin could be determined as stated by Zakaria et al. (2013). Hemicellulose started to decomposed at the absorption band of 1050 cm^{-1} and 1734 cm^{-1}, while cellulose takes place simultaneously on band 1050 cm^{-1} and at 1437 cm^{-1} which the C-H_2 bond was shearing. In extend, lignin was breakdown at lower

infrared bands of 891 cm^{-1} as well as at 1256 cm^{-1} and 1437 cm^{-1} which similar to the decomposition of cellulose but the bond was benched.
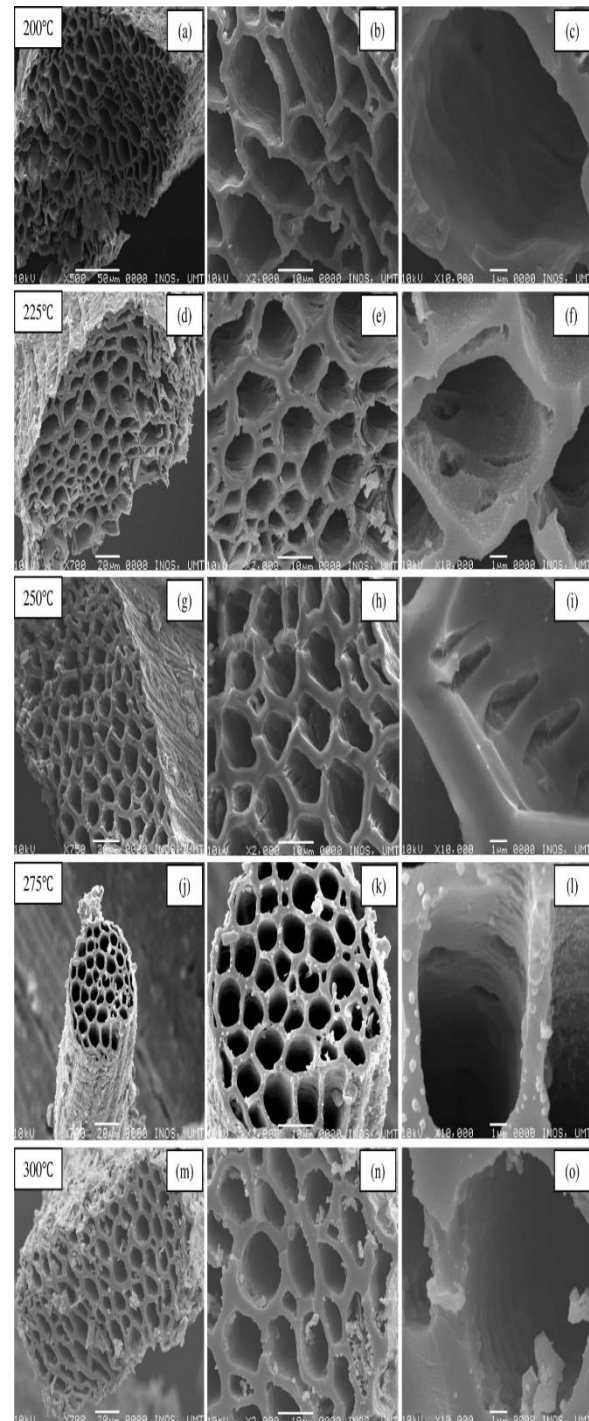

Fig. 4: Structure of torrefied EFB on 60 minutes of torrefaction at respective temperatures with magnifications of ×700 (a, d, g, j, m), ×2000 (b, e, h, k, n) and ×10000 (c, f, i, l, o)

Hemicellulose decomposed at a relatively long wavelength compared to cellulose and lignin because the hemicellulose does not require a longer time of torrefaction (60 minutes) to be deformed. It was already take place during 40 minutes of residence time at lower temperature, as could be seen in Fig. 3 by the formation of rupture structure. Meanwhile, for cellulose, the structure was degraded at relatively lower wavelength than of hemicellulose

indicating the process take place at high temperature alongside high residence time between 40 minutes up to 60 minutes. Since the structure of lignin was complex (Gomez et al., 2008), its deformation took place at a lower wavelength with not fully detached explaining that it required relatively high temperature of 250-500°c to be degraded whereby temperature above 300°c was for pyrolysis process (Chen and Kuo, 2011a). Thus, the degradation of lignin could only be appeared at lower wavenumbers. Longer residence time would cause lignocellulose to be decomposed. In other words, as the time of torrefaction increasing, the intensity of

bands whereby the degradation of hemicellulose took place was decreasing as mentioned in Figs. 3-7 respectively. It was not only for hemicellulose, both of cellulose and lignin were also affected by the time but not fully caused degradation to be happens.

Lignin which has been mention in previous paragraph did not fully detached its structure made the its band to showed only a slightly decrease in bands. Summary of FTIR analysis with respective functional groups presented on particulars bands associates with their compounds were stated in Table 1.
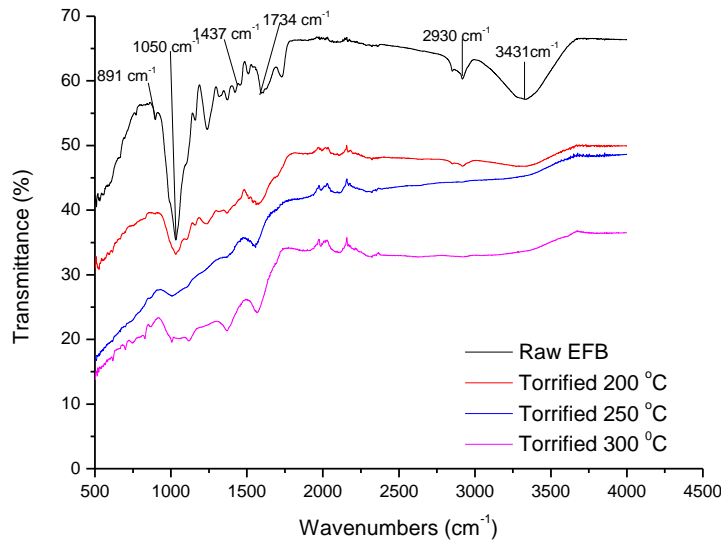

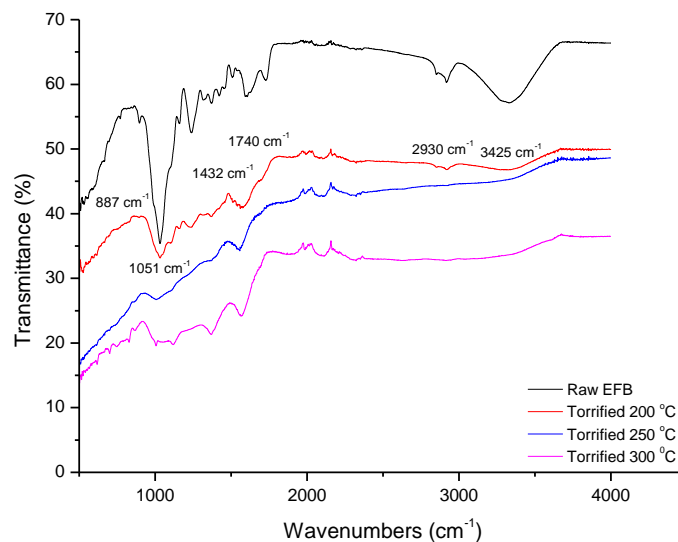**Fig. 5:** Functional groups presence during 20 minutes

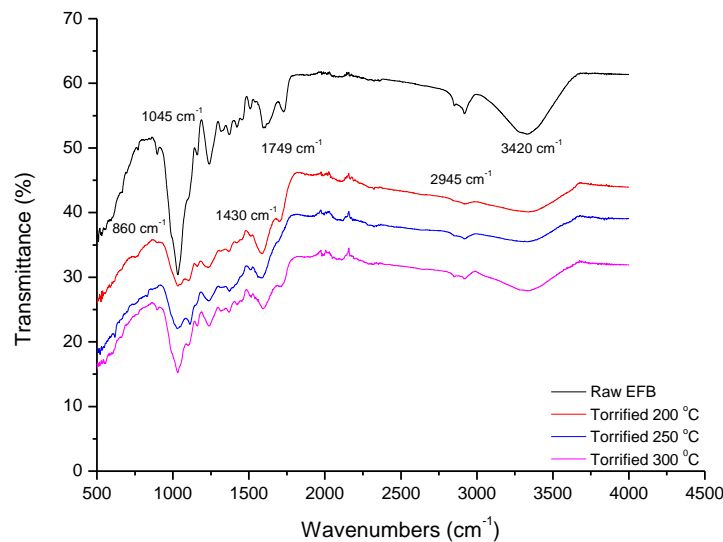**Fig. 6:** Functional groups presence during 40 minutes

Fig. 7: Functional groups presence during 40 minutes

4. Conclusion

Both morphology and bonding behaviour of the torrefied EFB were influenced the degradation of lignocellulose; hemicellulose, cellulose and lignin. Surface morphology of torrefied EFB showed at higher temperature, lignin was denatured compared to cellulose and hemicellulose. Hemicellulose was starting to degrade at lower temperature with medium residence time and completely destroyed as temperature increase whereas cellulose degraded at medium temperature as its structure was slightly complex than cellulose. Not only that, upon torrefaction takes place, the structures forming and became porous due to high released of moisture content made the structure dried out. All structures of torrefied EFB showed that the hemicellulose degraded at lower torrefaction temperature as well as its spectrum involving the C=O and C-O stretching bonds.

Meanwhile, cellulose decomposed at a medium temperature of torrefaction involving also C-O and C-H_2 bonds. Decomposition of lignin is hard to be determined based on the torrefied EFB's structures; fortunately the FTIR spectra proved it occurred at the band gap of 891, 1256 and 1437 cm^{-1}.

Table 1: FTIR functional groups present at particular wavenumbers with their compound

Wavenumber (cm^{-1})	Functional Group (Phenomenon)	Compound Class
3420-3435	O-H stretching	Phenols, alcohols
2930-2950	C-H and C-H_2 stretching	Alkanes
1730-1750	C=O stretching	Carbonyl (aldehydes, ketones, carboxylic acids)
1430-1440	C-H stretching, C-H_2 shearing and benching	Alkanes
1260	C-O-C stretching	Aromatics
1045-1055	C-O stretching	Esters, ethers
850-890	C-H bending (deformation)	Aromatics

Acknowledgment

References

Abdullah R, Rizman ZI, Dzulkefli NN, Ismail S, Shafie R, and Jusoh MH (2016). Design an automatic temperature control system for smart tudung saji using Arduino microcontroller. ARPN Journal of Engineering and Applied Sciences, 11(16): 9578-9581.

Ahmad MI, Alauddin ZA, Soid SN, Mohamed M, Rizman ZI, Rasat MS, Razab MK, and Amini MH (2015). Performance and carbon efficiency analysis of biomass via stratified gasifier.

ARPN Journal of Engineering and Applied Sciences, 10(20): 9533-9537.

Ahmad MI, Rasat MS, Soid SN, Mohamed M, Rizman ZI, and Amini MH (2016). Preliminary study of microwave irradiation towards oil palm empty fruit bunches biomass. Journal of Tropical Resources and Sustainable Science, 4: 133-137.

Awalludin MF, Sulaiman O, Hashim R, and Nadhari WN (2015). An overview of the oil palm industry in Malaysia and its waste utilization through thermochemical conversion, specifically via liquefaction. Renewable and Sustainable Energy Reviews, 50: 1469–1484.

Basu P (2013). Torrefaction. In: Basu P (Ed.), Biomass gasification, pyrolysis and torrefaction: Practical design and theory: 87–145. Academic Press, Cambridge, USA.

Bergman PC and Kiel JH (2005). Torrefaction for biomass upgrading. In the 14th European Biomass Conference and Exhibition, Paris, France, 17-21.

Chen WH and Kuo PC (2011a). Isothermal torrefaction kinetics of hemicellulose, cellulose, lignin and xylan using thermogravimetric analysis. Energy, 36(11): 6451–6460.

Chen WH and Kuo PC (2011b). Torrefaction and co-torrefaction characterization of hemicellulose, cellulose and lignin as well as torrefaction of some basic constituents in biomass. Energy, 36(2): 803–811.

Chen WH, Lu KM, and Tsai CM (2012). An experimental analysis on property and structure variations of agricultural wastes undergoing torrefaction. Applied Energy, 100: 318–325.

Cruz G, Ávila I, dos Santos AM, and Crnkovic PM (2012). Effects of torrefaction on biomass: A thermal and morphological evaluation. In the 14th Brazilian Congress of Thermal Sciences and Engineering, Rio de Janeiro, Brazil: 18-22.

Gomez LD, Steele-King CG, and McQueen-Mason SJ (2008). Sustainable liquid biofuels from biomass: The writing's on the walls. New Phytologist, 178(3): 473–485.

Hakeem KR, Jawaid M, and Alothman OY (2015). Agricultural biomass based potential materials. Springer International Publishing, Berlin, Germany.

Hamzah Z, Allias AA, Hashim O, and Lee BB (2013). Characterization of physicochemical properties of biochar from different agricultural residues. Advances in Environmental Biology, 7(12): 3752–3758.

Ibrahim RH, Darvell LI, Jones JM, and Williams A (2013). Physicochemical characterisation of torrefied biomass. Journal of Analytical and Applied Pyrolysis, 103: 21–30.

IEA (2010). Key world energy statistics 2010. International Energy Agency, Paris, France. Available online at: https://www.iea.org

Ismail K, Ishak MAM, Ab Ghani Z, Abdullah MF, Safian MTU, Idris SS, and Hakimi NINM (2013). Microwave-assisted pyrolysis of palm kernel shell: Optimization using response surface methodology (RSM). Renewable Energy, 55: 357–365.

Kassim MN, Idres M, Ahmad MI, and Rizman ZI (2015). Computational analysis of air intake system for internal combustion engine in presence of acoustic resonator. ARPN Journal of Engineering and Applied Sciences, 10(20): 9468-9475.

Koguleshun S, Fei LP, Nabihah S, Chin HC, and Shamala G (2015). Synthesis of oil palm empty fruit bunch (EFB) derived solid acid catalyst for esterification of waste cooking oils. Sains Malaysiana, 44(11): 1573–1577.

Law KN, Daud WR, and Ghazali A (2007). Morphological and chemical nature of fiber strands of oil palm empty-fruit-bunch (OPEFB). BioResources, 2(3): 351–362.

Loppinet SA, Aymonier C, and Cansell F (2008). Current and foreseeable applications of supercritical water for energy and the environment. ChemSusChem, 1(6): 486–503.

Mertke A and Aneziris CG (2015). The influence of nanoparticles and functional metallic additions on the thermal shock resistance of carbon bonded alumina refractories. Ceramics International, 41(1): 1541-1552.

Mohamed M, Amini MH, Sulaiman MA, Abu MB, Bakar MN, Abdullah NH, Yusuf NA, Khairul M, Razab AA, and Rizman ZI (2015). CFD simulation using wood (cengal and meranti) to improve cooling effect for Malaysia green building. ARPN Journal of Engineering and Applied Sciences, 10(20): 9462-9467.

Nasri NS, Hamza UD, Abdulkadir A, Siti Noraishah I, and Hamed MM (2013). Utilization of sustainable palm empty fruit bunch sorbents for carbon dioxide capture. In the 6th International Conference on Process Systems Engineering (PSE ASIA), Kuala Lumpur, Malaysia: 582-587.

Painuly JP (2001). Barriers to renewable energy penetration: A framework for analysis. Renewable Energy, 24(1): 73–89.

Pua FL, Fang Z, Zakaria S, Guo F, and Chia CH (2011). Direct production of biodiesel from high-acid value Jatropha oil with solid acid catalyst derived from lignin. Biotechnology for Biofuels, 4(1): 56-63.

Rizman ZI, Yeap KH, Ismail N, Mohamad N and Husin NH (2013). Design an automatic temperature control system for smart electric fan using PIC. International Journal of Science and Research, 2(9): 1-4.

Sathaye JA and Meyers S (2013). Greenhouse gas mitigation assessment: A guidebook. Springer Science and Business Media, Berlin, Germany.

Tumuluru JS, Sokhansanj S, Wright CT, and Boardman RD (2010). Biomass torrefaction process review and moving bed torrefaction system model development. Technical Report Number: INL/EXT-10-19569. Idaho National Laboratory (INL), Idaho Falls, USA. https://doi.org/10.2172/1042391

Uemura Y, Omar W, Othman NA, Yusup S, and Tsutsui T (2013). Torrefaction of oil palm EFB in the presence of oxygen. Fuel, 103: 156–160.

Wen JL, Sun SL, Yuan TQ, Xu F, and Sun RC (2014). Understanding the chemical and structural transformations of lignin macromolecule during torrefaction. Applied Energy, 121: 1–9.

Zakaria S, TzeKhong L, ChinHua C, FeiLing P, FanSuet P, Roslan R, and Amran UA (2013). Characterization of Fe2O3/FeOOH catalyzed solvolytic liquefaction of oil palm empty fruit bunch (EFB) products. Journal of Bioremediation and Biodegradation, 4(S4): 1–7.